Journal of Applied Polymer Science

Lignin-Xylaric Acid-Polyurethane-Based Polymer Network Systems: Preparation and Characterization

Helinä Pohjanlehto,[1] Harri M. Setälä,[1] Donald E. Kiely,[2] Armando G. McDonald[3]

[1]Technical Research Centre of Finland (VTT), Biologinkuja 7, FI-02044 Espoo, Finland

[2]Rivertop Renewables, P.O. Box 8165, Missoula, Montana 59807-8165

[3]Renewable Materials Program, Department of Forest, Rangeland and Fire Science, University of Idaho, Moscow, Idaho 83844-1132

Correspondence to: H. Pohjanlehto (E-mail: helina.pohjanlehto@vtt.fi)

ABSTRACT: Polyurethanes (PU) were synthesized from lignin by first preparing a prepolymer from esterified sugar-based trihydroxyl compound xylaric acid and a 20 mol % excess of methylene diphenyl diisocyanate. The prepolymer was crosslinked with 5, 10, and 15 wt % of an industrial soda lignin, and polyethylene glycol was used to bring soft segments into the material structure. The total amount of bio-based starting materials was as high as 35%. Evidence for the reaction between the prepolymer and lignin was observed using Fourier transform infrared spectroscopic analysis and ^{13}C nuclear magnetic resonance spectroscopy. The thermal properties of the materials were investigated by differential scanning calorimetry (DSC) and thermogravimetric analysis (TGA). The mechanical and viscoelastic properties of the materials were determined by dynamic mechanical analysis (DMA). The glass transition temperatures (T_g) obtained from DSC and DMA showed a trend of increasing T_g with the increasing amount of lignin. A similar trend was observed with TGA for the increasing thermal stability up to 550°C with the increasing amount of lignin. The lignin-polyurethanes obtained were stiff materials showing high Young's modulus values. © 2013 Wiley Periodicals, Inc. J. Appl. Polym. Sci. **2014**, *131*, 39714.

KEYWORDS: crosslinking; polyurethanes; polysaccharides

Received 12 February 2013; accepted 27 June 2013

DOI: 10.1002/app.39714

INTRODUCTION

The demand for renewable resources as starting materials in industrial syntheses has increased remarkably over recent years. Furthermore, the decreasing amount of fossil fuels is causing the search for alternatives that would minimize environmental impacts. Nonfood biomass based components such as lignocellulose materials are potentially promising materials for the preparation of polymeric materials because of their bio-based nature, biodegradability, low toxicity, and wide availability.

Lignin is the second most abundant polymer found in nature, constituting about 15–40 wt % of the dry matter of woody plants,[1] but only a small part of the total available amount is being commercially exploited. The incorporation of lignin into novel bio-based materials is recognized as one of the most viable approaches to accomplish its valorization. Lignin has been reported, for example, to improve the tensile strength,[2] thermal stability,[3] and biodegradability[4] of different polymers. Lignin has a polydisperse polyphenolic structure with many different functional groups that include hydroxyl, carboxyl, methoxy, and phenyl groups. Because of its interesting functional properties, lignin has potential for use in various applications and many different kinds of materials have been prepared.[1] The free hydroxyl groups are one of the most characteristic functions in lignin and they can be utilized as the polyol component, for example, in polyesters,[5] polyesteramides,[6] and in polyurethane synthesis. Lignin-PUs have been prepared from many starting materials, such as polyethylene glycol (PEG),[7] adipic acid,[8] polybutadiene, modified lignin reacted directly with isocyanates,[9,10] ε-caprolactone,[11] and carbon nanotubes.[12]

Xylaric acid is an aldaric acid prepared by oxidizing hemicellulose derived xylose with nitric acid.[13] The dicarboxylic acid functionality of xylaric acid has been utilized in a few polymerization reactions. For example, xylaric acid was modified to a diallyl monomer, *N, N′*-diallylxylardiamide, to be used as a crosslinker in xylan-based hydrogel synthesis.[14] The preparation of polyhydroxypolyamides from xylaric acid and other aldaric acids has also been investigated.[15–17] Xylaric acid also contains three secondary hydroxyl groups that can be utilized in a reaction with isocyanates to make polyurethanes. No former work combining aldaric acids with lignin using isocyanates has been

reported as yet but Marin et al.[18,19] used derivatives of the naturally occurring aldaric acid, tartaric acid, as the hydroxyl containing component when preparing linear PUs with isocyanates. Tartaric acid was also used in the preparation of a PU resin, [20] as a chiral component in azobenzene PUs,[21,22] as a chain extender in PU/organoclay nanocomposites,[23] and in meta kaolin filled PUs.[24] Other sugar-derived monomers have also been used in the preparation of PUs.[25–29]

The main goal of this study was to investigate the reaction between esterified xylaric acid-diisocyanate prepolymer with lignin. The pendant hydroxyl groups of xylaric acid in a reaction with a difunctional isocyanate form a network structure that can subsequently react with lignin to form an even more complex network structure. PEG was used as a compatibilizer in the reaction to bring soft segments into the polymer. The thermal and mechanical properties of the resulting materials were tested and compared to a reference material with no lignin.

EXPERIMENTAL

Materials

Commercial lignin (Protobind 1000) was obtained from ALM Private Limited, India (bimodal distribution, 1st peak M_w 210,000 g/mol and M_n 193,000 g/mol, and the 2nd peak M_w 88,800 g/mol and M_n 72,100 g/mol), and technical grade xylaric acid from Rivertop Renewables, Missoula, MT, USA. PEG average mol. wt. 1300–1600 g/mol (PEG-1540, JT Baker) was vacuum dried at +70°C before use. Other reagents (acetyl chloride (99+%, Acros Organics), methanol (HPLC grade, EMD), DMSO (99.9+% anhydrous, Aldrich), *N,N*'-dimethylformamide (DMF Extra Dry, 99.8%, Acros Organics), di-n-butyltin dilaurate (95%, Aldrich) and) were used as is. Methylene diphenyl diisocyanate (MDI, 99.5%, Acros Organics) was stored at −20°C and handled under an inert atmosphere.

General Methods

Fourier transform infrared (FTIR) spectroscopic analysis was performed using a ThermoNicolet Avatar 370 spectrometer operating in the attenuated total reflection (ATR) mode (SmartPerformer, ZnSe crystal). All spectra were recorded from 400 to 4000 cm^{-1} at a resolution of 4 cm^{-1}, an average of 64 scans, and the spectra ATR and baseline corrected. ^{1}H nuclear magnetic resonance (NMR) spectroscopy was performed on a Bruker Avance 300 spectrometer operating at 300.1 MHz using TMS as internal reference. ^{13}C NMR was performed on a Bruker Avance III spectrometer operating at 125.8 MHz. DMSO-d_6 was used as the NMR solvent. Differential scanning calorimetry (DSC) experiments were carried out at heating/cooling rates of 10°C/min on a TA Instruments model Q200 DSC equipped with a refrigeration cooling unit. Sample sizes of 4–7 mg were analyzed using a temperature profile from −80°C to +200°C collecting data from the second heating cycle. Thermogravimetric analysis (TGA) was carried out using a PerkinElmer TGA7 instrument to evaluate the thermal stability of the materials. Two to five mg of samples in platinum pans were heated at 20°C/min ramp rate in nitrogen atmosphere with a flow rate of 30 mL/min. TGA (weight loss as a function of temperature) and derivative thermogravimetry (DTG) curves were recorded from +50°C to +900°C. Dynamic mechanical analysis (DMA) experiments were performed using a TA Instruments model Q800 DMA. Specimens were tested in the tensile mode with a temperature ramp from+ 20°C to +150°C at 1 Hz and a heating rate of 3°C/min. Young's modulus was determined from the linear part of the stress–strain curves run for each of the samples. The degree of swelling (DS) of films in DMF was investigated by immersing the dried and weighed films in DMF and allowed to completely swell for 136 h to reach equilibrium swelling. The excess DMF was removed by tapping with filter paper and the swollen films were weighed. The DS was calculated according to the following equation:

$$\mathrm{DS}\,(\%) = \frac{W_s - W_d}{W_d} x100 \tag{1}$$

where W_s and W_d are the weights of the swollen and dried film, respectively. The densities of the PU films were obtained by measuring the dimensions of the samples. The crosslink densities (V_c) of the materials were calculated from the swelling and density measurements using the Flory-Rehner equation[2]:

$$V_c = -\frac{\ln(1-V_2) + V_2 + \chi V_2^2}{V_s d_r\left(V_2^{\frac{1}{3}} - \frac{V_2}{2}\right)} \tag{2}$$

where, V_s is the molar volume of solvent, V_2 is the volume fraction of polymer in swollen sample, d_r is the density of the polymer, and χ is the polymer–solvent interaction parameter (0.4).[30] The weight average molecular weight (M_w) of Protobind 1000 lignin as its acetyl ester derivative was determined by size exclusion chromatography (SEC).[31] Lignin was esterified and recovered according to Fox and McDonald.[32] Lignin acetate was dissolved in tetrahydrofuran (THF) at a concentration of 1 mg/mL and filtered (0.45 μm, PTFE syringe filter) prior to analysis. Separation was performed using a Jordi DVB linear mixed bed column (7.8 mm x 300 mm) coupled to a Water Breeze HPLC system with triple detection (Viscotek 270 detector and a Waters refractive index detector) on elution with THF at 0.5 mL/min. The SEC system was calibrated using a narrow polystyrene standard (M_w 99,000 g/mol) and data analyzed with OmniSEC.4.1 software. The M_w was corrected to take into account the increased weight of lignin by acetylation.

Preparation of Xylaric Acid

Xylaric acid was prepared by nitric acid oxidation of D-xylose employing a computer controlled reactor as recently reported by Hinton et al.[33]

Synthesis of Xylaric Acid Ester/Lactone (1a, 1b)

Xylaric acid was esterified according to literature.[15] Acetyl chloride (8.2 mL) was slowly added to methanol (250 mL) on an ice bath. Xylaric acid (47.9 g, 0.266 mol) was added to the solution and the reaction mixture was refluxed for 67 h. The solvent was evaporated, diluted with methanol (2 x 100 mL), and concentrated to a brown syrup. The yield of the xylaric acid diester/ester-lactone mixture (**1a, 1b**) was 51.8 g (94%). The ratio of 1a and 1b (3 : 2) was calculated as the ratio of aliphatic ester/lactone methoxy protons from ^{1}H NMR spectra (Figure 1), and this product mixture was used as such (XE).

1a. ^{1}H NMR (300 MHz, DMSO-d_6, δ): 4.12 (d, 2H, H-2 and H-4, $J_{2,3} = J_{3,4} = 4.4$ Hz), 3.90 (t, 1H, H-3), 3.64 (s, 6H, -OMe).

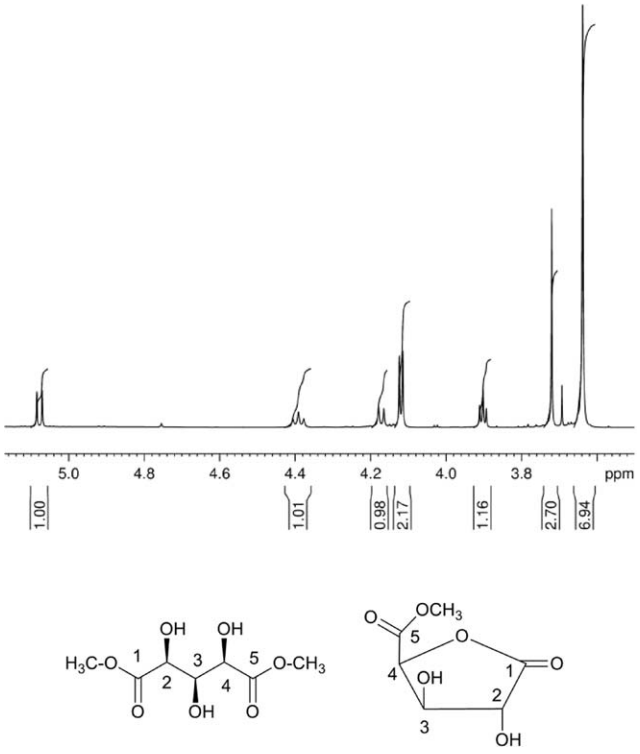

Figure 1. ^{1}H NMR spectrum of XE.

1b. ^{1}H NMR (300 MHz, DMSO-d_6, δ): 5.08 (d, 1H, H-4, $J_{3,4}$= $J_{2,3}$= 7.1 Hz), 4.39 (t, 1H, H-3), 4.17 (d, 1H, H-2), 3.72 (s, 3H, -OMe)

Synthesis of Lignin-PU's

The synthesis scheme of lignin-PUs is shown in Figure 2. XE was dissolved in a small amount of DMF in a 100-mL three-necked flask. A 20 mol % excess of MDI dissolved in a small amount of DMF and 1 mol % (MDI) of di-*n*-butyltin dilaurate catalyst were added under nitrogen atmosphere. After mixing for 10 min at +20°C 20 wt % of PEG was dissolved and mixed with lignin in DMF and added to the reaction mixture. The mixture was stirred for 15 min at +20°C, then heated to +50°C for 50–60 min, poured onto an aluminium foil pan, and placed in an oven for 24 h at +40°C. The films were soaked/washed with DMF for 24 h, then with acetone for 4 days and vacuum dried at +70°C for 2 days.

RESULTS AND DISCUSSION

Synthesis

XE and Protobind lignin (1.05 OH/C9)[34] have a large number of OH groups in their structures and are good candidates as polyol components in PU synthesis. The isocyanate groups of MDI react with the pendant secondary OH groups of XE forming a prepolymer network structure leaving the ester groups of XE unaffected. The prepolymer formed with an excess of MDI can be further crosslinked by adding lignin. The amount of lignin added was calculated by the weight ratio between lignin and total chemicals, i.e. XE, MDI, PEG and lignin. Different amounts of lignin were used and samples with 0, 5, 10, and 15 wt % lignin were named as L0, L5, L10, and L15, respectively. The sample with no lignin (L0) was used as the reference material. DMF was selected as solvent in the PU reaction as Protobind lignin was soluble in it. PEG can be used as a combatibilizer to bring soft segments to the polymer network.[35] The dosage of PEG was 20 wt % in all of the samples. Solution casting was selected as the appropriate method for the preparation of the PU films as the used components had a tendency to gel before completion of the reaction. No evidence of phase separation was observed upon curing and all the PU films obtained were optically clear and appeared to be homogeneous. The color of PU films varied from yellow to dark brown according to increasing lignin content.

Spectroscopic Characterization

FTIR was run for all the samples to confirm a successful reaction between the starting materials. FTIR spectra of XE, lignin, L0, and L15 are presented in Figure 3. It is clearly seen in the L15 spectrum that the OH bands from lignin and XE at 3406 and 3435 cm^{-1}, respectively, have decreased. This is an indication of the consumption of lignin and XE OH groups in reaction with MDI during polymerization. The new band at 3335 cm^{-1} was assigned to the hydrogen bonded NH bonds from the urethane linkage.[36] Broad bands around 2912 cm^{-1} in the L0 spectrum and 2920 cm^{-1} in the L15 spectrum are assigned to the CH_2 stretching of PEG[37] and MDI[38], and CH stretching of XE.[15] The band at 2920 cm^{-1} is additionally assigned to the CH and CH_2 stretching of lignin. The presence of lignin has shifted this band to a lower frequency and increased the intensity of the band. The band at 1735 cm^{-1} in L15 spectrum can be assigned to the absorption of carbonyl groups from XE and urethane –C=O. Aromatic functionalities of lignin were assigned to the peaks at 1601 and 1508 cm^{-1}.[47] The band at 1515 cm^{-1} is of higher intensity than the corresponding band in the lignin spectrum (1508 cm^{-1}), which indicates the presence of NH bonds from the urethane linkage in addition to lignin aromatic functionalities.[40] The band at 1209 cm^{-1} indicates the C-O-C ether bonds from lignin and PEG.[39] The incorporation of PEG can also be seen from the broad band at 1087 cm^{-1} which can be assigned to the asymmetric vibrations of -CH_2- in the PEG backbone.[41]

^{13}C NMR was run to confirm the results obtained from FTIR. A representative ^{13}C NMR spectrum of sample L5 is presented in Figure 4. Methoxy peaks from XE and lignin are found in the 50–55 ppm region and aliphatic C-O bonds from XE, PEG,

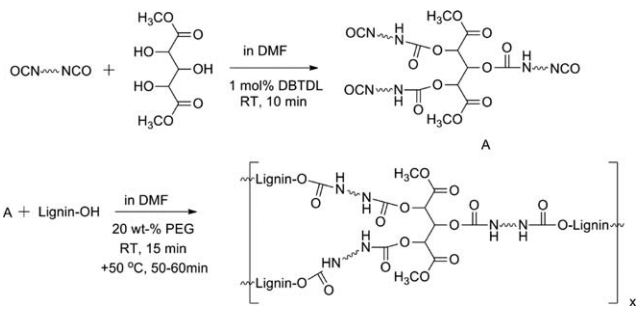

Figure 2. Schematic presentation of the preparation of lignin-PUs.

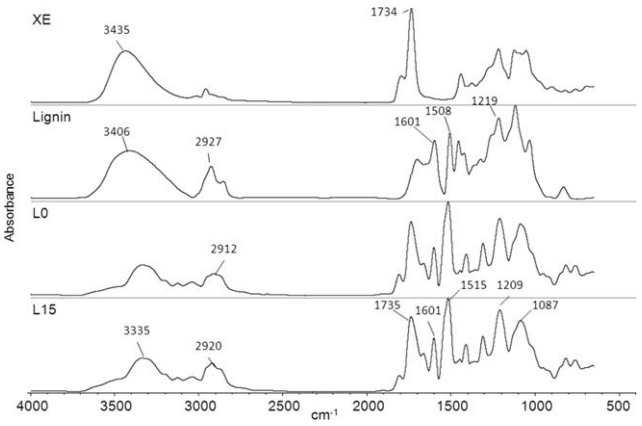

Figure 3. Comparison of the FTIR spectra of XE, lignin, L0, and L15.

and lignin in the 63–80 ppm region. Multiple peaks for aromatic functionalities are observed in the 117–155 ppm region. Carbon peaks from MDI and lignin aromatic rings are situated at 117–120 ppm, Ar-C peaks at 125–138 ppm, and Ar-O from lignin at 142–155 ppm. Aliphatic carbonyl group peaks for XE and lignin appear between 162 and 175 ppm. These peaks together with the results from FTIR indicate a successful reaction between the starting materials.[45]

Swelling Measurements and Crosslink Density

The swelling properties of the lignin-PU films were investigated by placing the dried films in an excess of DMF at room temperature. The crosslink densities were calculated using the measured density values and the results obtained from the swelling measurements. Figure 5 shows the degrees of swelling and the crosslink densities as a function of the amount of lignin in the samples. The sample L5 shows the highest absorbency (660%) after which the absorbency decreases as the amount of lignin increases, L10 having an absorbency of 469% and L15 an absorbency of 410%. The crosslink densities show the opposite behavior, as expected. L15 has the highest crosslink density ($0.153*10^{-3}$ mol/g) diminishing its absorbency. L5 has the lowest crosslink density ($0.026*10^{-3}$ mol/g) that explains its highest absorbing capacity and L10 similarly shows the same trend with a crosslink density of 0.078×10^{-3} mol/g. L0 shows the lowest absorbency (397%) and also a high crosslink density (0.151×10^{-3} mol/g) indicating that the reaction between XE, PEG, and the NCO groups of MDI without lignin produces the most tightly packed network structure diminishing the absorbency of DMF. This could also be because of more favorable hydrogen bonding between the side chains of these molecules where no lignin was present. When 5% lignin is added, the NCO groups also react with the hydroxyl groups of lignin resulting in a more loosely packed network and the DS increases. However, the trend was reversed when 10% and 15% lignin was added. This is because of the rising crosslink density and an augmentation in the hydrophobic component in the films owing to the increased amount of hydrophobic lignin. This is in accordance with work done with lignin-based PU hydrogels where the absorbency of the gels increased up to 35% of lignin and after that started decreasing.[4]

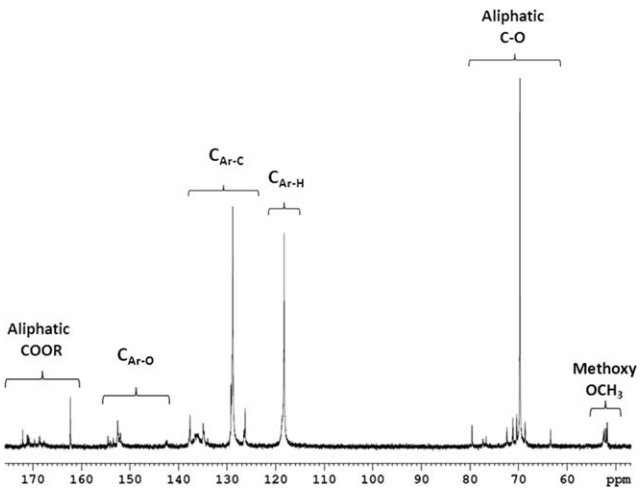

Figure 4. ^{13}C NMR spectrum of L5.

Thermal and Mechanical Properties

DSC and DMA were used to measure the thermal and mechanical properties of the samples (Table I). The loss modulus (E'') peak maximum temperature from DMA measurements was taken as the T_g of the materials and compared to the T_g values obtained from DSC. The same trend was observed with the T_g's obtained from both analysis methods, DMA giving values about 20% lower than DSC as expected.[42] A DSC thermogram of L15 is shown in Figure 6 as a representative thermogram. DSC was run at a wider temperature range than DMA and two T_g's for each sample were found indicating different zones in the material. The first T_g from all of the samples was found in the -20^oC region. This could result from adjacent PEG chains that form a localized semi-crystalline structure that softens around -20^oC. The second T_g was found to be dependent on the amount of lignin. The T_g of the control sample L0 was the lowest (94.8^oC) and the T_g of L15 the highest (132.4^oC). The addition of lignin increases the crosslink density and the formation of a compact network structure[7] which is in accordance with the results obtained from the crosslink density calculations (Figure 5). L0 has a high crosslink density but a low T_g indicating that lignin increases the T_g of the materials whereas crosslink density does not. The lignin used in this study, Protobind 1000, was measured to have a T_g of 173.3^oC which is higher

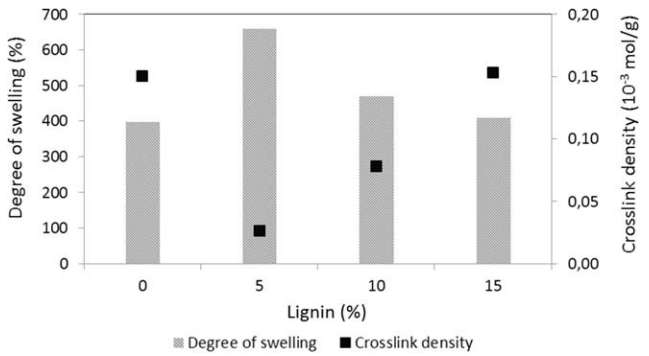

Figure 5. The degree of swelling and the crosslink density for L0, L5, L10 and L15.

Table I. Glass Transition Temperature and Young's Modulus for Samples with 0–15 wt % Lignin

Sample	Lignin (%)	T_{g1},°C (DSC)	T_{g2},°C (DSC)	T_g,°C (DMA)	E' (MPa) at 20°C	Young's modulus (GPa)
L0	0	−21.9	94.8	80	2000	1.45
L5	5	−20.9	112.4	95	1930	1.53
L10	10	−22.6	127.5	98	1560	1.69
L15	15	−23.1	132.4	106	1380	2.12

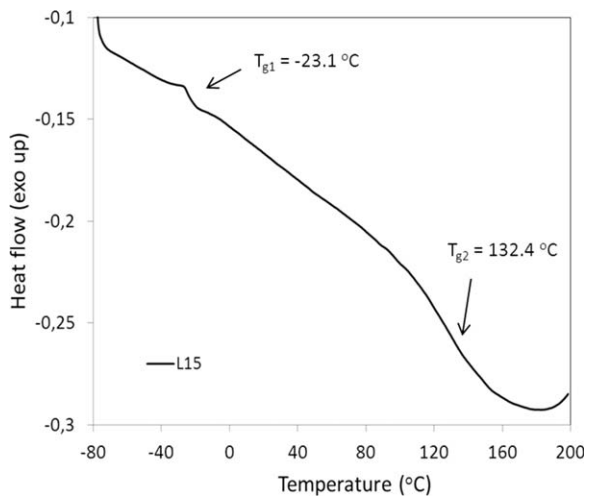

Figure 6. DSC thermogram for L15.

than any of the T_g's obtained for the PU's indicating homogeneous network structures in the PU's.

Lignin-PUs were subjected to DMA analysis to determine their stiffness (Young's modulus) (Table I) and viscoelastic properties. The storage modulus (E') and E'' are plotted as a function of temperature in Figures 7 and 8, respectively. The Young's modulus values (1.45 GPa for L0 to 2.12 GPa for L15) increase when the amount of aromatic rings from lignin in the structure increases leading to chain stiffness. This behavior is in good agreement with the previous results.[43,44] However, the E' values for the samples show a reversed trend. E' normally increases with the amount of lignin when preparing thermoplastic polymers.[5,45] However, it was observed that the prepared lignin-PU networks became more brittle (higher Young's modulus) with the increasing amount of lignin and the crosslink density that evidently reduced the elastic portion of the materials. Room temperature, 20°C, was chosen to represent the decreased E' upon increased lignin content (Table I). For example, L5 showed E'=1930 MPa, while L15 had decreased to E'=1380 MPa. E' begins to decrease with increasing temperature because of the relaxation of the polymer chains and decreases more rapidly as the materials enter their glass transition. E' for L0 (981 MPa) at its T_g temperature has decreased 51%. E' for L5 is 932 MPa and for L10 and L15 621 and 490 MPa, respectively, corresponding to decreases of 52%, 60% and 65%.

The E'' thermograms show a clear trend for the T_g's of the polymers (Table I). L0 has the lowest T_g at 80°C with the highest E'' value of 170 MPa. L5 and L10 showed increasing T_g's (95°C and 98°C) and reached E'' values of 128 and 129 MPa, respectively, whereas L15 had the lowest value of 107 MPa with the highest T_g at 106°C. The E'' decreases as the amount of lignin increases indicating a reduction in the viscous part of the polymer when lignin is incorporated into the network system.

The effect of lignin's presence and content on the stability of the materials was studied by means of thermogravimetry. Figure 9 shows the residual mass as a function of temperature for each of the samples and Figure 10 shows the derivative curves for the same samples. In general, the thermal stability of the samples increases when lignin is present up to about 550°C

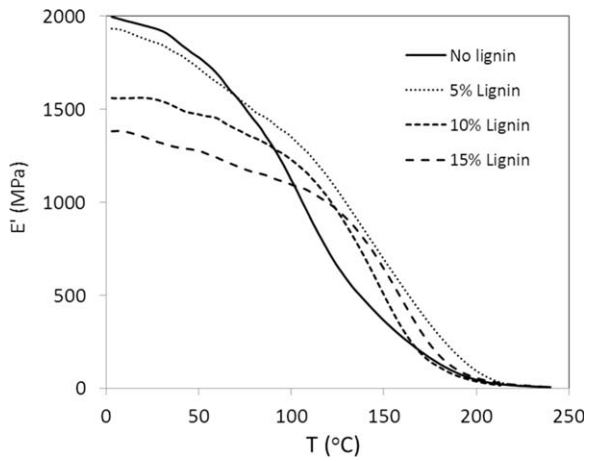

Figure 7. The effect of lignin content and temperature on storage modulus (E').

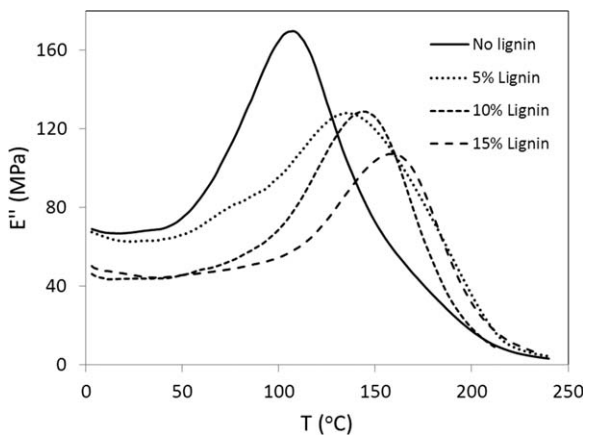

Figure 8. The effect of lignin content and temperature on loss modulus (E'').

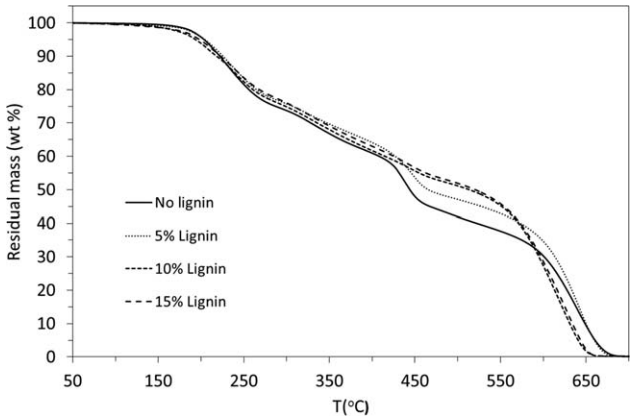

Figure 9. Weight loss of L0, L5, L10, and L15.

(Figure 9). In this study, the peak temperature of TG derivatives was used as an indication of the decomposition temperature (Figure 10). All the samples show a four-stage degradation process (Table II). The weight losses for the first and second steps follow the same tendency for all the samples suggesting that a common decomposition mechanism must be operating in such stages. The first stage starting at 190°C corresponds to the dissociation of the weakest bonds in the PU resulting in the degradation of the urethane bonds. The slower degradation at the second stage (300–380°C) and at the third stage (380–480°C) for L10 and L15 correspond to the degradation of PEG soft segments, which is in accordance with literature.[46] However, the rate of the dissociation in stage three for L0 and L5 is remarkably higher. This could be explained with a larger amount of attached PEG in the L0 and L5 structures because no competitive lignin or only a small amount (5 wt %) is present. The fourth stage (480–700°C) corresponds to the degradation of aromatic moieties. The thermal decomposition temperature at the fourth stage starting at 500°C for L10 and L15 and at 550°C for L0 and L5 decreased with the samples with more lignin. The amount of char residue in all the samples is negligible probably because of the high amount of methoxyl, hydroxyl and carboxyl groups in the sample structures resulting in volatile decomposition products.[47,48]

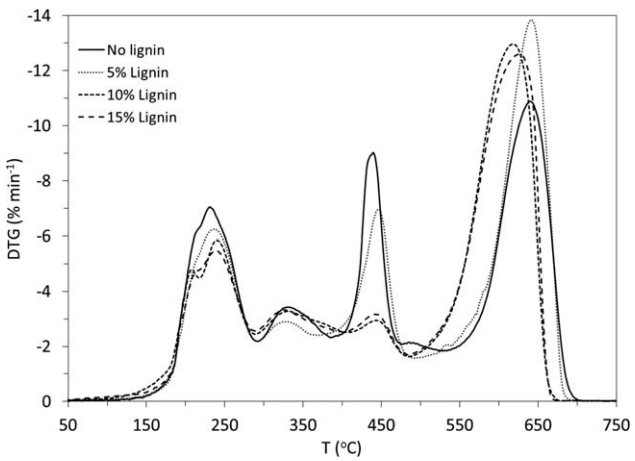

Figure 10. The DTG curves for L0, L5, L10, and L15.

Table II. Major Degradation Temperatures for L0, L5, L10, and L15

	Major degradation temperatures (°C)			
Sample	1st	2nd	3rd	4th
L0	234	327	442	641
L5	240	327	446	642
L10	240	331	441	617
L15	239	325	445	627

CONCLUSIONS

A series of lignin-xylaric acid PU's were prepared through the network-forming reaction between plant-derived esterified xylaric acid and lignin using MDI as a coupling agent, PEG as a compatibilizer and di-*n*-butyltin dilaurate as a catalyst in dry DMF. The content of bio-based materials in the final products was as high as 35 wt %. The material properties could be modulated by changing the amount of lignin. With the increasing amount of lignin Young's modulus of 2.12 GPa and T_g of 128°C was reached when 15 wt % lignin was present suggesting that lignin acted as a reinforcing agent. Similarly, the TGA showed that the incorporation of lignin increased the thermal stability of the materials. This makes them possible candidates for material applications that require stable thermal conditions such as electrical components.

ACKNOWLEDGMENTS

This work was supported by the (i) Academy of Finland through the Finnish Centre of Excellence in White Biotechnology-Green Chemistry–project and (ii) USDA-NIFA Wood Utilization Research grant number 2010–34158-20938. The authors would like to thank Liqing Wei for help with DMA.

REFERENCES

1. Doherty, W. O. S.; Mousavioun, P.; Fellows, C. M. *Ind. Crop. Prod.* **2011**, *33*, 259.
2. Sarkar, S.; Adhikari, B. *Eur. Polym. J.* **2001**, *37*, 1391.
3. Sarkar, S.; Adhikari, B. *Polym. Degrad. Stab.* **2001**, *73*, 169.
4. Peng, Z.; Chen, F. *Int. J. Polym. Mater.* **2011**, *60*, 674.
5. Sivasankarapillai, G.; McDonald, A. G. *Biomass Bioenergy* **2011**, *35*, 919.
6. Sivasankarapillai, G.; McDonald, A. G.; Li, H. *Biomass Bioenergy* **2012**, *47*, 99.
7. Chahar, S.; Dastidar, M. G.; Choudhary, V.; Sharma, D. K. *J. Adhes. Sci. Technol.* **2004**, *18*, 169.
8. Ciobanu, C.; Ungureanu, M.; Ignat, L.; Ungureanu, D.; Popa, V. I. *Ind. Crop. Prod.* **2004**, *20*, 231.
9. Chung, H.; Washburn, N. R. *Appl. Mater. Interfaces* **2012**, *4*, 2840.
10. Bonini, C.; D'Auria, M.; Emanuele, L.; Ferri, R.; Pucciariello, R.; Sabia, A. R. *J. Appl. Polym. Sci.* **2005**, *98*, 1451.

11. Hatakeyama, T.; Izuta, Y.; Hirose, S.; Hatakeyama, H. *Polymer* **2002**, *43*, 1177.
12. Faria, F. A. C.; Evtuguin, D. V.; Rudnitskaya, A.; Gomes, M. T. S. R.; Oliveira, J. A. B. P.; Graca, M. P. F.; Costa, L. C. *Polym. Int.* **2012**, *61*, 788.
13. Kiely, D. E.; Carter, A.; Shrout, D. P. U.S. Pat. 5,599,977, (**1997**).
14. Pohjanlehto, H.; Setälä, H.; Kammiovirta, K.; Harlin, A. *Carbohydr. Res.* **2011** *346*, 2736.
15. Kiely, D. E.; Chen, L.; Lin, T.-H. *J. Polym. Sci. Part A: Polym. Chem.* **2000**, *38*, 594.
16. Morton, D. V.; Kiely, D. E. *J. Appl. Polym. Sci.* **2000**, *77*, 3085.
17. Kiely, D. E.; Kramer, K.; Zhang, J. U.S. Pat. 6,894,135, (**2005**).
18. Marín, R.; Martínez de Ilarduya, A.; Muñoz-Guerra, S. *J. Polym. Sci. Part A: Polym. Chem.* **2009**, *47*, 2391.
19. Marín, R.; Muñoz-Guerra, S. *J. Polym. Sci. Part A: Polym. Chem.* **2008**, *46*, 7996.
20. Gündüz, G.; Idlibi, Y.; Akovali, G. *J. Coat. Technol.* **2002**, *74*, 59.
21. Liu, J.; Qiu, F.; Cao, G.; Shen, Q.; Cao, Z.; Yang, D. *J. Appl. Polym. Sci.* **2011**, *121*, 2567.
22. Qiu, F.; Zhang, W.; Yang, D.; Zhao, M.; Cao, G.; Li, P. *J. Appl. Polym. Sci.* **2010**, *115*, 146.
23. Melinte, V.; Buruiana, T.; Mihai, A.; Buruiana, E. C. *High Perform. Polym.* **2011**, *23*, 238.
24. Roopa, S.; Siddaramaiah. *J. Reinforc. Plast. Compos.* **2007**, *26*, 681.
25. Begines, B.; Zamora, F.; Benito, E.; Garcia-Martin, M. G.; Galbis, J. A. *J. Polym. Sci. Part A: Polym. Chem.* **2012**, *50*, 4638.
26. De Paz, M. V.; Marin, R.; Zamora, F.; Hakkou, K.; Alla, A.; Galbis, J. A.; Muñoz-Guerra, S. *J. Polym. Sci. Part A: Polym. Chem.* **2007**, *45*, 4109.
27. Yamanaka, C.; Hashimoto, K. *J. Polym. Sci. Part A: Polym. Chem.* **2002**, *40*, 4158.
28. Prömpers, G.; Keul, H.; Höcker, H. *Green Chem.* **2006**, *8*, 467.
29. Hashimoto, K.; Yaginuma, K.; Nara, S.; Okawa, H. *Polym. J.* **2005**, *37*, 384.
30. Cateto, C. A. B.; Barreiro, M. F. F.; Rodrigues, A. E.; Belgacem, M. N. XXI Encontro Nacional da TECNICELPA / VI CIADICYP **2010**, 12-15 Outubro 2010, Lisboa, Portugal.
31. Steward, D.; McDonald, A. G.; Meder, A. R. Proceedings of the 6th Pacific Rim Biobased Composites Symposium, Portland, Oregon (November 10–13), **2002**, pp 584.
32. Fox, S. C.; McDonald, A. G. *BioRes.* **2010**, *5*, 990.
33. Hinton, M. R.; Manley-Harris, M.; Hardcastle, K. I.; Kiely, D. E. *J. Carbohydr. Chem.* **2013**, *32*, 68.
34. Malutan, T.; Nicu, R.; and Popa, V. I. *BioRes.* **2008**, *3*, 13.
35. Saraf, V. P.; Glasser, W. G.; Wilkes, G. L.; McGrath, J. E. *J. Appl. Polym. Sci.* **1985**, *30*, 2207.
36. Cateto, C. A.; Barreiro, M. F.; Rodrigues, A. E.; Belgacem, M. N. *React. Funct. Polym.* **2011**, *71*, 863.
37. Jagadish, R. S.; Raj, B.; Parameswara, P.; Somashekar, R. *J. Appl. Polym. Sci.* **2013**, DOI: 10.1002/APP.37616.
38. Delpech, M. C.; Miranda, G. S. *Cent. Eur. J. Eng.* **2012**, *2*, 231.
39. Gierlinger, N.; Goswami, L.; Schmidt, M.; Burgert, I.; Coutand, C.; Rogge, T.; Schwanninger, M. *Biomacromolecules* **2008**, *9*, 2194.
40. Lopes, R. V. V.; Osorio, L. F. B.; Santos, M. L.; Sales, M. J. A. *Macromol. Symp.* **2012**, *319*, 173.
41. Yang, J.; Gao, J. C. *Mater. Sci. Technol.* **2008**, *24*, 261.
42. Menard, K. P. In Dynamic Mechanical Analysis: A Practical Introduction; CRC Press; Boca Raton, FL, **1999**; p 102.
43. Hatakeyama, H.; Hatakeyama, T. *Macromol. Symp.* **2005**, *224*, 219.
44. Yoshida, H.; Mörck, R.; Kringstad, K. P.; Hatakeyama, H. *J. Appl. Polym. Sci.* **1987**, *34*, 1187.
45. Saito, T.; Brown, R. B.; Hunt, M. A.; Pickel, D. L.; Pickel, J. M.; Messman, J. M.; Baker, F. S.; Keller, M.; Naskar, A. K. *Green. Chem.* **2012**, DOI:10.1039/c2gc35933b.
46. Chattopadhyay, D. K.; Webster, D. C. *Prog. Polym. Sci.* **2009**, *34*, 1068.
47. Sahoo, S.; Seydibeyoglu, M. Ö.; Mohanty, A. K.; Misra, M. *Biomass Bioenergy* **2011**, *35*, 4230.
48. Jakab, E.; Faix, O.; Tiii, F. *J. Anal. Appl. Pyrolysis* **1997**, *40–41*, 171.